Interferon Regulatory Factor 6 Is Necessary for Salivary Glands and Pancreas Development

K.A. Metwalli, M.A. Do, K. Nguyen, S. Mallick, K. Kin, N. Farokhnia, G. Jun, and W.D. Fakhouri

Appendix

Materials and Methods

βgal staining of transgenic mice

To identify the spatiotemporal expression of IRF6 in the craniofacial region, IRF6 expression was observed using transgenic mice that possessed the reporter gene *LacZ* driven by the human *IRF6* enhancer element. Activity of the IRF6 enhancer element was visualized by staining transgenic specimens for beta-galactosidase, which stain tissues with blue color. For whole mount and cryosection specimens, 4 transgenic embryos at different developmental time points were processed as previously described (Fakhouri et al. 2010).

Histological staining procedures

To characterize the *Irf6* null phenotype, different histological stains were applied to salivary gland and pancreas tissues. Sectioned tissues from 10 wild type and 10 *Irf6* null embryos were stained following either hematoxylin and eosin (H&E), or Alcian blue and nuclear fast red, or Alcian blue and Periodic Acid Schiff (PAS) staining protocols. H&E staining was performed as previously described (Fakhouri et al. 2010). Alcian blue and nuclear fast red staining stains mucins in blue and nuclei in pink, and aids in visualization of the distribution of these substances. Alcian blue and Periodic Acid Schiff demonstrates the presence of glycogen and mucin protein in purple, acid mucins in blue, neutral mucins in magenta, mixed mucous in bluish purple, and nuclei in dark blue.

Salivary gland explants and culture

For ex-vivo organ culture, a pair of submandibular glands of murine embryos at E13.5 stage was extracted. Pregnant females were euthanized with CO_2, followed by cervical dislocation to collect murine embryos. After the isolation, the embryos were immediately placed in 1X phosphate buffer solution (PBS) to remove excess blood and maintain electrolyte homeostasis of embryos. The mandible of each embryo was dissected from the head at the level of mouth and further extraction of the submandibular glands was carried under the dissection microscope. The two submandibular glands were isolated in the sac from the rest of the remaining tissue portion. The submandibular glands were cultured on a Millipore membrane submerged in a DMEM medium solution with 3% FBS + transferrin + vitamin C. The explants were incubated in 5% CO2 incubator at 37°C for 4 days and the count of the end buds of submandibular and sublingual glands was performed using a Nikon stereomicroscope.

Immunohistochemistry (IHC) and Immunofluorescent (IF) Staining

Immuno-staining was used to qualitatively determine the protein expression pattern and level in the *Irf6* null mutant salivary gland tissues compared to wild type tissues. IHC staining was performed for embryos at E17.5 using ΔN-P63 antibodies (1:150, Abcam, MA) and MIST1 (1:250. GeneTex). DAB chromogen was used on the sections and then counter stained with Mayer's Hematoxylin to visualize nuclei. IF was performed to visualize the presence of IRF6, P63, and activated-Caspase 3 (CASP3) in salivary gland tissues at E15.5 and E17.5. Bromodeoxyuridine (BrdU), a thymidine analog that is incorporated into DNA during the S phase of the cell cycle, was used to detect proliferating cells. Four biological replicates of each wild type and *Irf6* null embryos were used for each immune-staining technique. Selected sections were deparaffinized and rehydrated as previously described (Fakhouri et al. 2014). The primary antibodies used were: polyclonal rabbit anti-Irf6, rabbit anti-casp3**,** mouse anti-ΔN-P63 **(**Ab735, Abcam, MA), BrdU (Abcam, MA). The secondary antibodies used were goat

anti-rabbit (A21429, Molecular Probes, CA) and goat anti-mouse (A11029, Molecular Probes, CA). Cell nuclei were marked with DAPI (D3571, Invitrogen, CA).

RNA-Seq of *Irf6* null salivary gland tissues

Illumina HiSeq2500 platform in a 2x100bp paired-end configuration was used to obtain 32 million reads on average for each library sample, and the analysis of differentially expressed genes (DEGs) was performed using edgeR package. Normalized read count (NRC) by the total read counts per sample were converted to log counts per million (log CPM) metrics and the differentially expressed genes in *Irf6* null salivary gland compared to wild type littermate were considered statistically different if the p-value is less than $<10^{-5}$ and the false-discovery rate (FDR) for multiple testing using Benjamini-Hochberg correction was less than <0.05. The sex of embryos used to extract salivary gland was retrospectively determined in each individual sample by exploring the expression of Xist which supposed to be silent in males (Appendix Table 2). For generating a heat map for each RNA-seq sample, the clustered image maps (CIM) function in the mixOmics R package was applied to cluster the 168 DEGs. This package uses hierarchical agglomerative clustering (HAC) with complete linkage based on Euclidean distance between expressed genes, i.e. the square root of the log CPM levels for each value in each individual samples. The top 19 differentially expressed genes with positive log CPM values either for both mutants or wild types with FDR<0.05 clustered closer together in the dendogram of the heat map.

RTqPCR and immunoblot

Total RNA was extracted from salivary gland tissues of *Irf6* null and wild type murine embryos to measure expression level of cellular markers *CD31*, *K7*, *K5*, *Srpr3*, *Tfap2a*, *Muc4* and *P53* as well as differentially expressed genes identified by RNA-seq data *Col9a2*, *Lect1*, *Matn1*, *Matn3*, *Hoxb6*, *Ereg*, *Tpo* and *Ltbp4* genes. RTqPCR experiments were performed as previously described (Fakhouri et al. 2010) using the SYBR Green Kit (Applied Biosystems, Foster City, CA, USA). Immunoblotting was performed in extracts from WT and *Irf6* null salivary gland tissues at P0 to detect the total protein levels of IRF6 and P53. Odyssey Li-Cor system was used to visualize the protein bands, and beta-actin was used as a loading control.

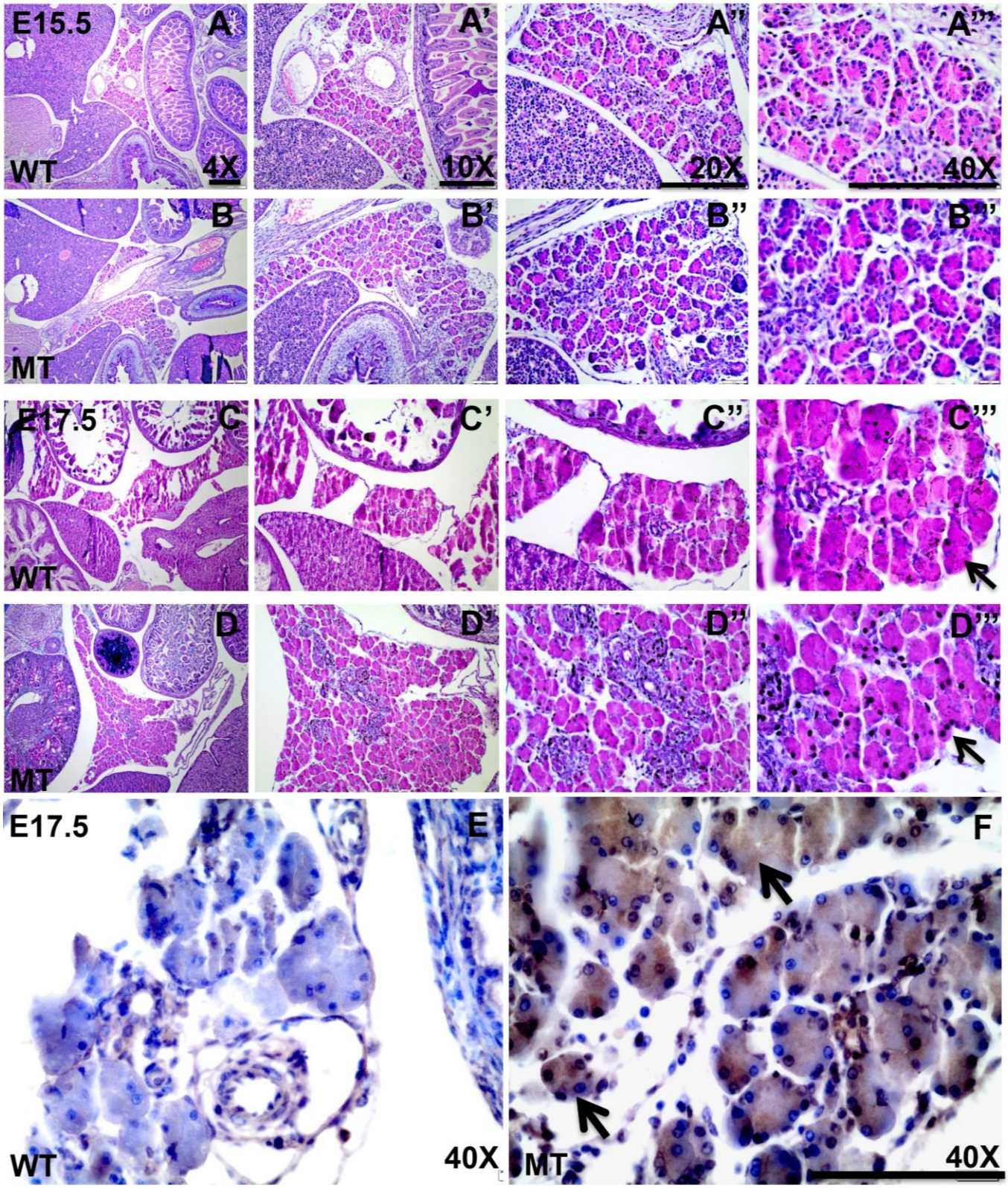

Appendix Figure 1. H&E and IHC staining of wild type (WT) and *Irf6* null (MT) pancreas at different developmental stages. No morphological changes are observed in wild type and Irf6 null pancreas at E15.5 (A, B series), although the number of stained nuclei is increased in *Irf6* null compared to WT at E17.5 (C, D series). Expression of MIST1 was detected in pancreas by IHC. MIST1 expression was subtle in wild type and detected mainly in nucleus of acinar cells (E). In *Irf6* null pancreas, elevated level of MIST1 was observed in the cytosol and nucleus of acinar cells at E17.5 (F).

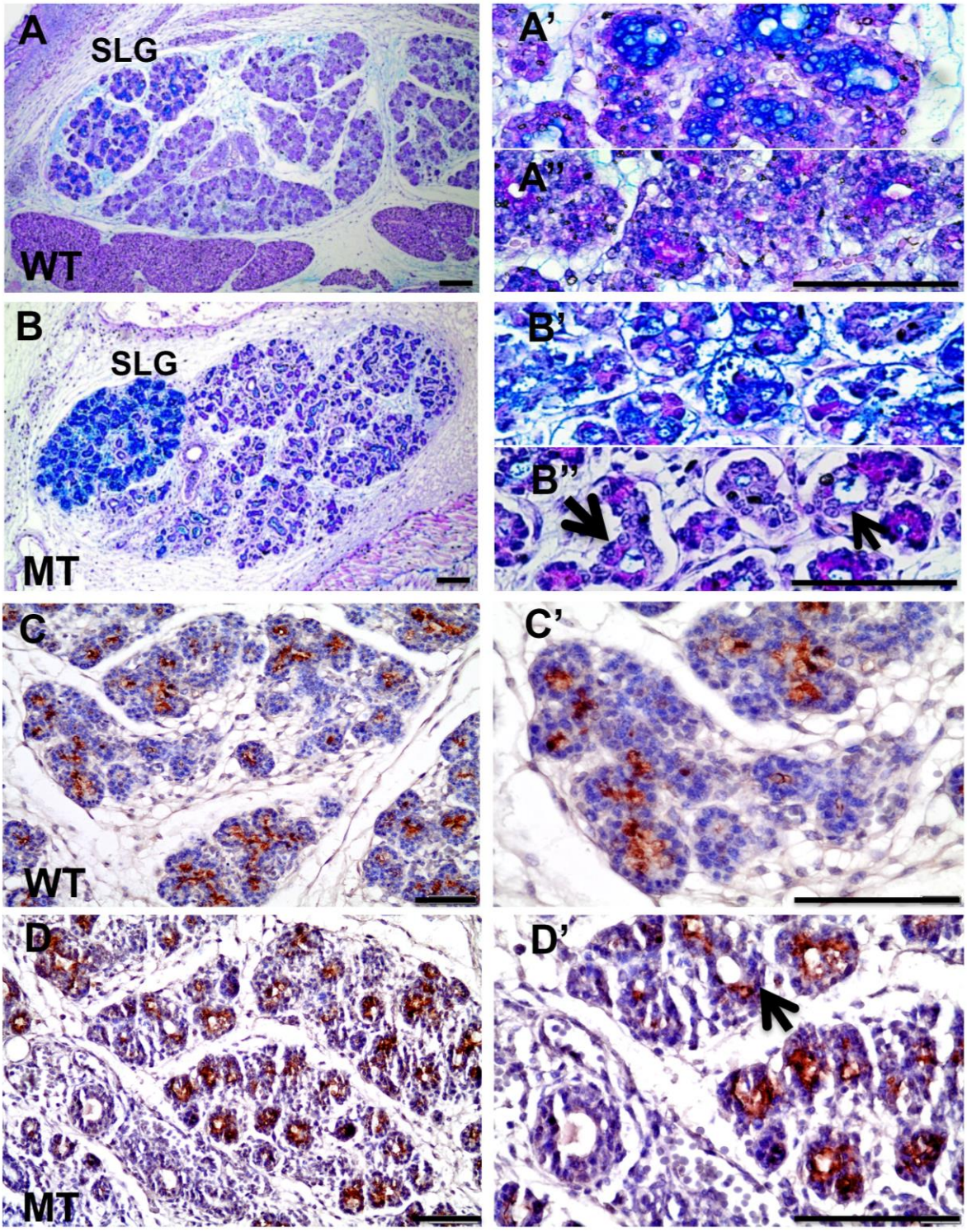

Appendix Figure 2. Histological and immuno-staining of wild type (WT) and *Irf6* null (MT) submandibular glands at E17.5. In wild type tissue, the blue staining of mucous acinii of sublingual gland (SLG) is distinct from the mix of the serous- and mucous-type acinii of submandibular gland (A series). Although the blue staining of mucous acinii is observed in *Irf6* null SLG (B), the organization and localization of the blue staining in mucous acinii are distrusted and abnormal (B',B"). Expression of the acinar differentiation marker MIST1 was investigated in salivary gland sections and shows apical localization in cytosol and nuclear localization in acinar cells in wild type tissues (C, C'). In *Irf6* null sections, MIST1 expression is more intense in the cytosol and nucleus of acinar cells (D). No apical localization in the cytosol is detected (D'). Scale bars are 150μm.

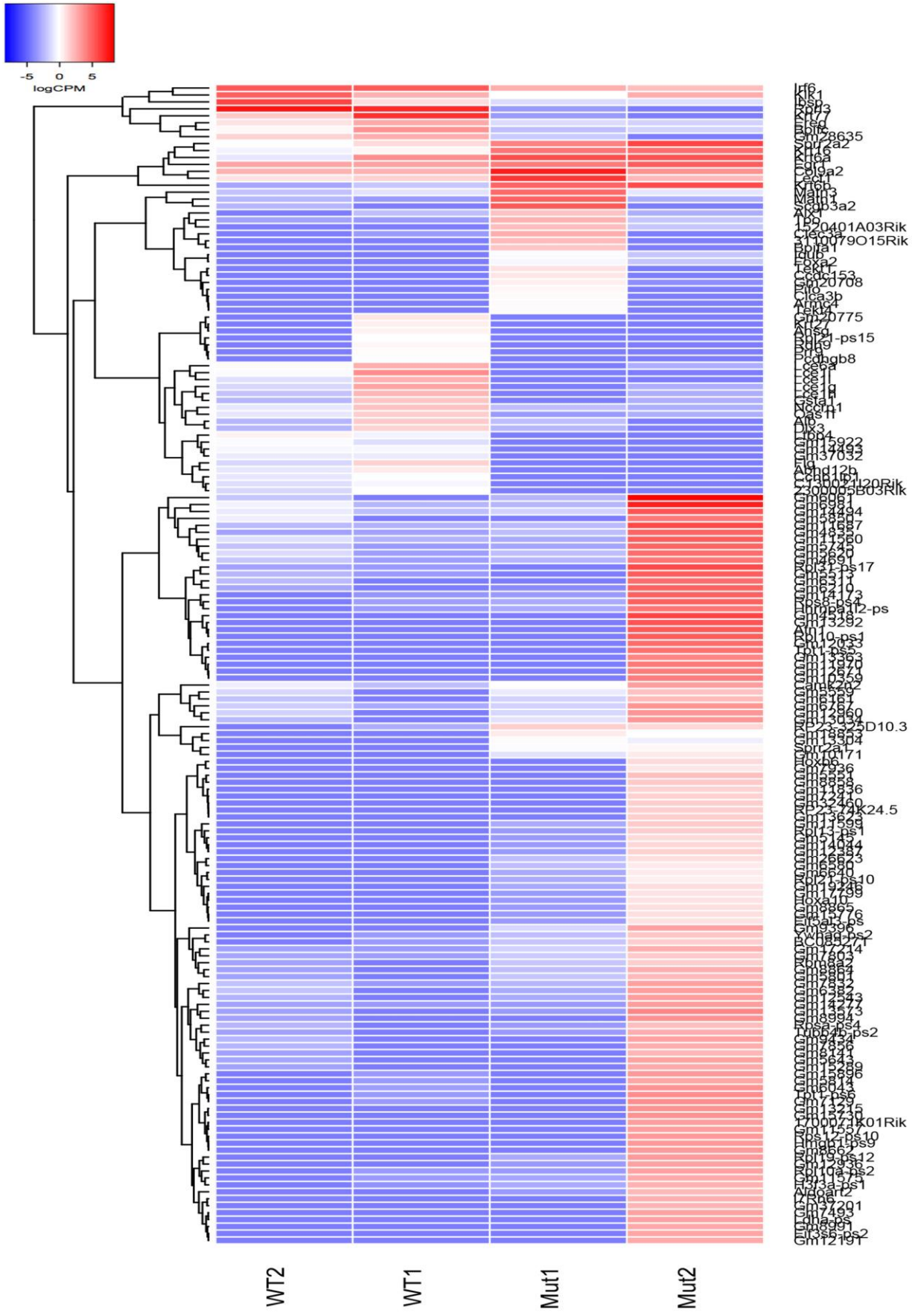

Appendix Figure 3. Heat map of the 168 significantly differentially expressed genes in Irf6 null embryos (MT1 and MT2) and their corresponding expression profile in wild type littermate embryos

(WT1 and WT2). Blue blocks represents genes that have decreased in expression, while red represents genes that have increased in expression. White represents no change in expression. The two mutant embryos have very obvious differences in gene expression when looking at the entire transcriptome. Even though both animals were the same sex and ostensibly the same stage (E14.5), it is possible that Mut2 is a different stage than Mut1. Nevertheless we identified differentially expressed genes (N = 168 with greater than 2 fold difference in gene expression levels), many of whom were validated with qPCR.

Appendix Table 1. A gene ontology of 168 differentially expressed genes in Irf6 null salivary gland at E14.5. The bioinfomatics program DAVID grouped genes into function categories. The table displays the top 7 functional categories, the number of genes from the 168 genes that fell into each category, a p-value corresponding to the functional significance of the genes in a given category, and Benjamini correction values. The functional categories of the current RNA-Seq data nicely overlap with the functional categories of microarray RNA expression that was performed in Irf6 null embryonic skin at E17.5 compared to WT littermates (Ingraham et al. 2006).

Function Annotation	Bar	Gene Count	P-value	Benjamini
Ribonucleoprotein		16	1.4E-13	2.1E-11
Ectoderm Development		7	3.7E-5	1.1E-2
Spliceosome		6	8.5E-5	1.8E-3
Skeletal System Development		8	3.7E-4	4.2E-2
Transmembrane Transporter Activity		3	8.0E-4	2.6E-2
EGF		6	1.1E-2	3.4E-1
Transcription Regulatory Activity		11	3.1E-2	5.0E-1

Appendix Table 2. Sex determination of the RNA-seq samples used in this study. Sex of embryonic samples was determined by calculating the total number of mapped reads to chromosomes X and Y and the expression level of Xist gene. Xist gene is supposed to be expressed only in females.

Chr	Chr Length	Female Control Sample	WT1	MT1	WT2	MT2
ChrX	171031299	1957898	1494836	1388440	820250	917986
ChrY	91744698	53620	146726	179630	76376	109140
X coverage		0.011447601	0.008740131	0.008118046	0.004795906	0.005367357
Y coverage		0.000584448	0.001599286	0.001957933	0.000832484	0.001189606
X/Y		19.58703206	5.465021206	4.146232277	5.760958022	4.511879472
Xist (TPM)		44.65	0.02	0.02	0	0.01